

EFFECTIVE COMPRESSIVE SENSING VIA REWEIGHTED TOTAL VARIATION AND WEIGHTED NUCLEAR NORM REGULARIZATION

Mingli Zhang¹, Christian Desrosiers¹, Caiming Zhang^{2,3}

¹ Software and IT Engineering department, École de technologie supérieure, Montreal, Canada, H3C 1K3

² Shandong Provincial Key Laboratory of Digital Media Technology, Jinan 250014, China

³ School of Computer Science and Technology, Shandong University, Jinan 250100, China

ABSTRACT

Total variation (TV) and non-local patch similarity have been used successfully to enhance the performance of compressive sensing (CS) approaches. However, such techniques can often remove important details in the image or introduce reconstruction artifacts. This paper presents a novel CS method, which uses an adaptive reweighted TV strategy to better preserve image edges. Our method also leverages the redundancy of non-local image patches through the use of weighted low rank regularization. An optimization strategy based on the ADMM algorithm is used to reconstruct images efficiently. Experimental results show our method to outperform state-of-the-art CS approaches, for various sampling ratios.

Index Terms— Compressive sensing, Total variation, Reweighted TV, Non-local self similarity, Low rank, ADMM.

1. INTRODUCTION

Compressive (or *compressed*) sensing (CS) has been widely exploited in image processing, with numerous applications in photography [1], video [2], spectral imaging [3] and medical imaging [4, 5]. The key idea of this technique is that, if the sampling matrix satisfies a condition known as the restricted isometry property (RIP), a sparse signal can be accurately reconstructed from undersampled measurements [6–8]. Formally, the model for reconstructing an image $x \in \mathbb{R}^n$ from measurements $y \in \mathbb{R}^m$ can be formulated as

$$y = \Phi x + \nu, \quad (1)$$

where $\Phi \in \mathbb{R}^{m \times n}$ is a known measurement operator, and ν is additive noise (e.g., Gaussian, Rice, etc.).

In most CS methods, the task of recovering x is defined as an inverse problem:

$$\hat{x} = \operatorname{argmin}_x \frac{1}{2} \|\Phi x - y\|_2^2 + \lambda \Psi(x), \quad (2)$$

where $\Psi(x)$ is a regularization prior, and λ is a parameter controlling the trade-off between data fidelity and the regularization of x . Generally, the regularization prior is based on the principle that x is sparse under some suitable transform such as wavelets [9]. Another popular regularization approach is total variation (TV) [9, 10], which is represented as:

$$\operatorname{TV}(\nabla x) = \sum_{i=1}^n \sqrt{(\nabla_1 x_i)^2 + (\nabla_2 x_i)^2}. \quad (3)$$

Because this approach penalizes gradients uniformly, it may result in the loss of image details like edges. To overcome this problem, a reweighted TV model was proposed in [7], where the gradient of a pixel i is penalized according to a weight w_i , i.e.

$$\operatorname{TV}(\nabla x, w) = \sum_{i=1}^n w_i \sqrt{(\nabla_1 x_i)^2 + (\nabla_2 x_i)^2}. \quad (4)$$

Weights w are updated iteratively from x in such a way that regions with sharp gradients (e.g., edges) are less penalized than uniform ones:

$$w_i^{t+1} = \frac{1}{\|\nabla x_i^t\|_2 + \epsilon}, \quad (5)$$

where ϵ is a small positive constant.

Another strategy to improve reconstruction is to exploit the redundancy of local patterns in the image, represented as small patches of pixels [11–14]. In this strategy, groups of similar patches are regularized by applying a sparsifying transform, for instance based on wavelets [13] or dictionary learning [14]. Similar patches can also be regularized using the fact that matrices having these patches as columns or rows have a low-rank [12, 15]. While CS methods based on patch similarity can significantly improve the reconstruction when few samples are available, they also have the tendency to over-smooth images by “averaging” similar patches [16].

Motivated by the aforementioned observations, we present a novel CS method based on reweighted TV and weighted low-rank regularization of similar patches. The main contributions of our work are as follows:

This work is supported by ÉTS, FRQNT (210057) and National Natural Science Foundation of China (61272431, 61373080).

1. The proposed method is, to our knowledge, the first one to combine reweighted TV and weighted nuclear norm regularization in a single model. As shown in our experiments, our method outperforms state-of-the-art CS approaches by providing a more accurate reconstruction;
2. We also present an innovative reweighting strategy for TV, in which only the most important image gradients are considered. Compared to the reweighted TV approach of [7], our strategy produces images having less reconstruction artifacts;
3. Finally, an efficient optimization technique, based on the Alternating Direction Method of Multipliers (ADMM) algorithm, is proposed to reconstruct an image from sparse measurements.

The rest of this paper is organized as follows. In Sections 2 and 3, we present our CS image recovery model and the optimization process used to reconstruct images. Section 4 then evaluates the proposed method on several benchmark images. Finally, we conclude the paper by summarizing the contributions and results of this work.

2. THE PROPOSED RECONSTRUCTION MODEL

We first present our novel reweighting strategy for TV, and then describe how this model can be enhanced by adding a regularization of similar patches based on the weighted nuclear norm.

2.1. TV reweighting strategy

In some cases, the reweighting approach described in Eq. (4) and (5) can incorporate low-frequency information from smooth regions in the gradient regularization. An example of this can be seen in Fig. 1(a), where noticeable gradient magnitudes are found in uniform regions corresponding to the woman's face and hand. As shown in our experiments, this problem may lead to the introduction of false textures and edge-like artifacts in the reconstructed image.

To avoid this problem, we propose a new reweighting strategy, inspired by the pre-processing technique used in [17] for the super-resolution problem. The key idea of our strategy is to decompose the current gradient image ∇x^t into a smooth (i.e., low frequency) component Y^t and a residual component Z^t , the latter used to define the TV weights. The smooth component can be obtained by solving the following deconvolution problem:

$$\operatorname{argmin}_Y \|\nabla x^t - f_{\text{low}} \otimes Y\|_2^2 + \kappa \sum_d \|g_d \otimes Y\|_2^2. \quad (6)$$

In this formulation, f_{low} is low pass filter of size 3×3 and $g_d = [1, -1]$ is the gradient operator along direction $d \in \{1 =$

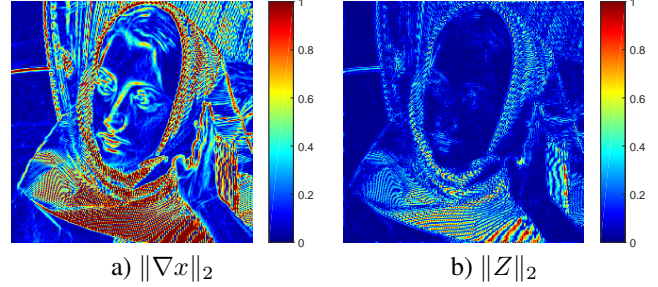


Fig. 1. (a) Gradient magnitudes and (b) residual component magnitudes.

horizontal, 2 = vertical}. The solution to this problem can be obtained efficiently using the FFT operator \mathcal{F} , i.e.

$$Y^t = \mathcal{F}^{-1} \left(\frac{\overline{\mathcal{F}(f_{\text{low}})} \circ \mathcal{F}(\nabla x^t)}{\overline{\mathcal{F}(f_{\text{low}})} \circ \mathcal{F}(f_{\text{low}}) + \kappa \sum_d \overline{\mathcal{F}(g_d)} \circ \mathcal{F}(g_d)} \right), \quad (7)$$

where “ $\bar{\cdot}$ ” is the complex conjugate operator, “ \circ ” the component-wise multiplication, “ \div ” the component-wise division, and κ is a user-defined parameter. The residual component is then obtained as

$$Z^t = \nabla x^t - f_{\text{low}} \otimes Y^t. \quad (8)$$

Finally, Z^t is used to update TV weights as follows:

$$w_i^{t+1} = \frac{1}{\|Z_i^t\|_2 + \epsilon}. \quad (9)$$

Figure 1(b) shows the magnitudes of the residual component obtained by Eq (8). We can see that smooth regions like the woman's face and hand have smaller values than the gradient magnitudes of Fig. 1(a).

2.2. Weighted nuclear norm regularization

As in most non-local self similarity (NSS) approaches [12, 15, 18, 19], we use a patch based model to reconstruct x . Let $p_i \in \mathbb{R}^d$ be the $\sqrt{d} \times \sqrt{d}$ patch centered on pixel i , and define as S_i the patch selection matrix such that $p_i = S_i x$. Note that patches from neighbor pixels overlap, thereby adding robustness to the reconstruction process. Moreover, let P_i be the matrix having as columns the k most similar patches to p_i , k being a user-defined parameter.

We exploit the redundancy of similar patches using a low-rank regularization approach. To avoid losing fine details in the reconstruction process, we approximate the rank of similar patch matrices using the weighted nuclear norm [18]: $\text{WNN}(P) = \sum_j \omega_j \sigma_j$, where σ_j is the j -th singular value of P such that $\sigma_j \leq \sigma_{j+1}$, and ω_j is its corresponding weight. Because larger singular values typically encode more meaningful information than smaller ones, following [18], we define weights ω_j so that components corresponding to larger singular values have less shrinkage, i.e. $\omega_j = 1/(\sigma_j + \epsilon)$, where ϵ is a small positive constant to avoid division by zero.

2.3. Combined regularization model

Combining the proposed reweighted TV model with the weighted nuclear norm regularization of similar patches, the image recovery task can be formulated as the following optimization problem:

$$\begin{aligned} \operatorname{argmin}_x \quad & \frac{1}{2} \|y - \Phi x\|_2^2 + \lambda \operatorname{TV}(\nabla x, w) + \gamma \sum_{i=1}^n \operatorname{WNN}(P_i) \\ \text{s.t.} \quad & p_i = S_i x, \quad i = 1, \dots, n. \end{aligned} \quad (10)$$

Here, λ and γ are user-defined parameters controlling the trade-off between data fidelity, reweighted TV regularization, and weighted nuclear norm regularization. The following section presents an efficient technique to solve this problem.

3. RECOVERING THE IMAGE

To recover image x in Eq. (10), we use an iterative optimization strategy based on the Alternating Direction Method of Multipliers (ADMM) algorithm [20]. This algorithm separates a hard-to-solve problem into several sub-problems, by introducing constrained auxiliary variables $z = \nabla x$ and $Q_i = P_i$, $i = 1, \dots, n$, and reformulating the problem as:

$$\begin{aligned} \operatorname{argmin}_{\substack{x, z, Q_i \\ a_i, B_i, c}} \quad & \frac{1}{2} \|y - \Phi x\|_2^2 + \lambda \operatorname{TV}(z, w) + \gamma \sum_{i=1}^n \operatorname{WNN}(Q_i) \\ & + \frac{\mu_A}{2} \sum_{i=1}^n \|p_i - S_i x + a_i\|_2^2 + \frac{\mu_B}{2} \sum_{i=1}^n \|Q_i - P_i + B_i\|_2^2 \\ & + \frac{\mu_C}{2} \|z - \nabla x + c\|_2^2 \end{aligned} \quad (11)$$

Here, a_i , B_i , $i = 1, \dots, n$, and c are the Lagrangian multipliers of each constraint, and μ_A , μ_B , μ_C are the corresponding meta-parameters. In practice, ADMM approaches are not very sensitive to the choice of these meta-parameters, which mostly affect the convergence of the solution [20].

Since the cost function of Eq. (11) is convex with respect to each parameter, we can optimize it by updating each parameter iteratively until convergence is reached. Assuming all other parameters are fixed, image x can thus be updated by solving the following problem:

$$\begin{aligned} \operatorname{argmin}_x \quad & \frac{1}{2} \|y - \Phi x\|_2^2 + \frac{\mu_A}{2} \sum_{i=1}^n \|p_i - S_i x + a_i\|_2^2 \\ & + \frac{\mu_C}{2} \|z - \nabla x + c\|_2^2, \end{aligned} \quad (12)$$

the solution of which is given by

$$\begin{aligned} x = & \left(\Phi^\top \Phi + \mu_A \sum_{i=1}^n S_i^\top S_i + \mu_C \nabla^\top \nabla \right)^{-1} \\ & \left(\Phi^\top y + \mu_A \sum_{i=1}^n S_i^\top (p_i + a_i) + \mu_C \nabla^\top (z + b) \right). \end{aligned} \quad (13)$$

Algorithm 1: The proposed CS method

Input: The measurements y and sampling matrix Φ ;
Output: The reconstructed image x ;

Initialize x using DCT based CS ;
Set $w_i := 1$, $a_i := 0$, $B_i := \mathbf{0}$, $i = 1, \dots, n$, $c := 0$;

while not converged do

Extract patches p_i from x ;
Find groups of similar patches P_i for each pixel i ;
Update Q_i , $i = 1, \dots, n$, using Eq. (15);
Update z , by solving Eq. (17);
Update image x using Eq. (13);
Update w using Eq. (9);
Update Lagrangian multipliers using Eq. (18);

return x ;

Because the matrix to invert is fixed, it can be factorized offline with Cholesky factorization. After this pre-processing step, x can be updated efficiently through backward/forward substitution [21]. Moreover, when Φ is orthogonal (e.g., Fourier transform), the system becomes block tridiagonal and can be solved in linear time using a generalized Thomas algorithm [22].

The task of updating Q_i , $i = 1, \dots, n$, corresponds to the following problem:

$$\operatorname{argmin}_{Q_i} \lambda \operatorname{WNN}(Q_i) + \frac{\mu_B}{2} \|Q_i - (P_i - B_i)\|_F^2. \quad (14)$$

This problem can be solved using the weighted singular value thresholding operator [18]:

$$Q_i = U \cdot \left(\Sigma - \frac{\lambda}{\mu_B} \operatorname{Diag}(\omega) \right)_+ \cdot V^\top, \quad (15)$$

where $U \Sigma V^\top$ is the SVD decomposition of $P_i - B_i$ and $(\cdot)_+ = \max\{\cdot, 0\}$.

To update the gradient auxiliary variable z , we consider the following problem

$$\operatorname{argmin}_z \lambda \operatorname{TV}(z, w) + \frac{\mu_C}{2} \|z - (\nabla x - c)\|_2^2. \quad (16)$$

Let $u_i = \nabla x_i - c_i$, this problem can be solved independently for each pixel i via group shrinkage:

$$z_i = \left(\sqrt{u_{i1}^2 + u_{i2}^2} - \frac{\lambda}{\mu_C} \right)_+ \cdot \frac{u_i}{\sqrt{u_{i1}^2 + u_{i2}^2}}. \quad (17)$$

Finally, the Lagrangian multipliers can be updated following the standard ADMM approach:

$$\begin{aligned} a_i^{t+1} &= a_i^t + (p_i^t - S_i x^t), \quad i = 1, \dots, n, \\ B_i^{t+1} &= B_i^t + (Q_i^t - P_i^t), \quad i = 1, \dots, n, \\ c^{t+1} &= c^t + (z^t - \nabla x^t). \end{aligned} \quad (18)$$



Fig. 2. The six benchmark images used in our experiments.

The whole reconstruction process is summarized in Algorithm 1.

4. EXPERIMENTS

We evaluate the proposed method on the six benchmark images of Fig. 2 and compare it to standard TV reconstruction [23], as well as two state-of-the-art CS approaches: NL-RCS [12], and SAISTCS [15]. The implementation of these approaches were obtained from their authors' website^{1,2}. The performance of the four tested methods was measured using Peak Signal to Noise Ratio (PSNR) and Structure Similarity Index (SSIM) [24].

Table 1. Mean accuracy (\pm stdev), in terms of PSNR (db) and SSIM, obtained by the tested methods for different sampling ratios. Values correspond to the average computed over the six images of Fig.2.

Sampling ratio	TV	NLRCS	SAISTCS	OURS
15 %	23.79 \pm 1.54 0.704 \pm 0.038	26.24 \pm 2.19 0.890 \pm 0.034	27.61 \pm 2.51 0.922 \pm 0.011	28.12 \pm 2.63 0.930 \pm 0.008
20 %	28.61 \pm 2.54 0.783 \pm 0.042	36.18 \pm 3.61 0.954 \pm 0.019	37.73 \pm 2.28 0.965 \pm 0.009	38.20 \pm 1.86 0.969 \pm 0.009
25 %	30.77 \pm 2.64 0.833 \pm 0.036	39.33 \pm 2.65 0.973 \pm 0.006	40.04 \pm 1.57 0.975 \pm 0.004	40.43 \pm 1.37 0.976 \pm 0.004
30 %	32.65 \pm 3.07 0.870 \pm 0.038	41.10 \pm 2.16 0.979 \pm 0.005	41.24 \pm 1.61 0.979 \pm 0.005	41.58 \pm 1.37 0.980 \pm 0.007

Our method's parameters were tuned using a different set of images, and set as follows: 6×6 for the patch size, $k = 45$ for the number of similar patches, $\lambda = 1.8$ and $\gamma = 0.9$ for the trade-off parameters, and $\kappa = 50$ for the TV reweighting strategy. The ADMM parameters were set empirically to $\mu_A = \mu_B = \mu_C = 1$.

Table 1 gives the mean reconstruction accuracy, in terms of PSNR and SSIM, obtained by the tested methods on the six benchmark images, for different numbers of random samples (measured as the ratio between the number of samples and total number of pixels). We see that our method outperforms all other approaches, for every sampling ratio and performance metric. Based on a paired Wilcoxon signed-rank test, these results are significant in all but four combinations of sampling ratio and accuracy metric, with $p < 0.05$. The advantage of our method over competing approach is particularly important for low sampling ratios, suggesting the use-

¹<http://see.xidian.edu.cn/faculty/wsdong/>

²<http://www.csee.wvu.edu/~xinl/>

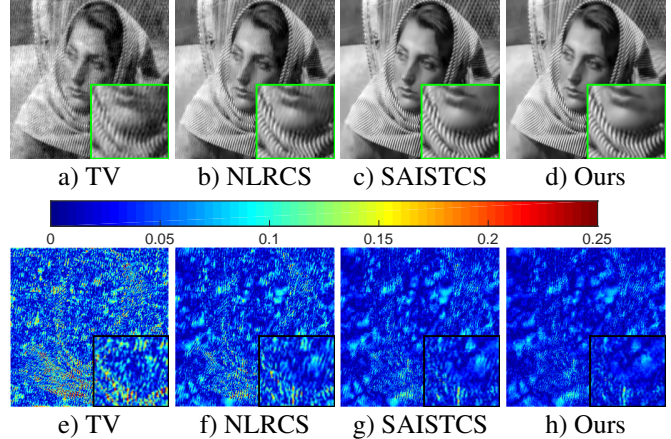


Fig. 3. Example of reconstructed images and residual errors obtained by the tested methods for a sampling ratio of 15%.

fulness of combining the reweighted TV and patch similarity regularization priors.

Figure 3 shows an example of reconstructed images and residual errors obtained by the tested methods for a sampling ratio of 15%. We observe that the proposed method leads to fewer reconstruction artifacts than other CS approaches. Moreover, our method provides a more accurate reconstruction of textured regions, such as the one showed in the zoomed area.

5. CONCLUSION

We presented a novel compressive sensing method that combines reweighted TV and the weighted nuclear norm regularization of similar patches in a single model. This method uses an innovative TV reweighting strategy, which reduces reconstruction artifacts by removing low frequency information. An efficient optimization strategy, based on the ADMM algorithm, was proposed to recover the image from under-sampled measurements. Experiments on benchmark images have shown our method to outperform state-of-the-art CS approaches, for various sampling ratios.

6. REFERENCES

- [1] Gang Huang, Hong Jiang, Kim Matthews, and Paul Wilford, "Lensless imaging by compressive sensing," in *2013 IEEE International Conference on Image Processing*. IEEE, 2013, pp. 2101–2105.
- [2] Yasunobu Hitomi, Jinwei Gu, Mohit Gupta, Tomoo Mitunaga, and Shree K Nayar, "Video from a single coded exposure photograph using a learned over-complete dictionary," in *2011 International Conference on Computer Vision*. IEEE, 2011, pp. 287–294.

- [3] Carlos A Hinojosa, Claudia V Correa, Henry Arguello, and Gonzalo R Arce, "Compressive spectral imaging using multiple snapshot colored-mosaic detector measurements," in *SPIE Commercial+ Scientific Sensing and Imaging*. International Society for Optics and Photonics, 2016, pp. 987004–987004.
- [4] Michael Lustig, David L Donoho, Juan M Santos, and John M Pauly, "Compressed sensing mri," *IEEE Signal Processing Magazine*, vol. 25, no. 2, pp. 72–82, 2008.
- [5] Mingli Zhang, Kuldeep Kumar, and Christian Desrosiers, "A weighted total variation approach for the atlas-based reconstruction of brain mr data," in *Image Processing (ICIP), 2016 IEEE International Conference on*. IEEE, 2016, pp. 4329–4333.
- [6] Emmanuel J Candes and Terence Tao, "Near-optimal signal recovery from random projections: Universal encoding strategies?," *Information Theory, IEEE Transactions on*, vol. 52, no. 12, pp. 5406–5425, 2006.
- [7] Emmanuel J Candes, Michael B Wakin, and Stephen P Boyd, "Enhancing sparsity by reweighted l_1 minimization," *Journal of Fourier analysis and applications*, vol. 14, no. 5-6, pp. 877–905, 2008.
- [8] David L Donoho, "Compressed sensing," *Information Theory, IEEE Transactions on*, vol. 52, no. 4, pp. 1289–1306, 2006.
- [9] Shiqian Ma, Wotao Yin, Yin Zhang, and Amit Chakraborty, "An efficient algorithm for compressed mr imaging using total variation and wavelets," in *Computer Vision and Pattern Recognition, 2008. CVPR 2008. IEEE Conference on*. IEEE, 2008, pp. 1–8.
- [10] Zhen Tian, Xun Jia, Kehong Yuan, Tinsu Pan, and Steve B Jiang, "Low-dose CT reconstruction via edge-preserving total variation regularization," *Physics in medicine and biology*, vol. 56, no. 18, pp. 5949, 2011.
- [11] José V Manjón, Pierrick Coupé, Antonio Buades, Vladimir Fonov, D Louis Collins, and Montserrat Robles, "Non-local MRI upsampling," *Medical image analysis*, vol. 14, no. 6, pp. 784–792, 2010.
- [12] Weisheng Dong, Guangming Shi, Xin Li, Yi Ma, and Feng Huang, "Compressive sensing via nonlocal low-rank regularization," *IEEE Transactions on Image Processing*, vol. 23, no. 8, pp. 3618–3632, 2014.
- [13] Xiaobo Qu, Yingkun Hou, Fan Lam, Di Guo, Jianhui Zhong, and Zhong Chen, "Magnetic resonance image reconstruction from undersampled measurements using a patch-based nonlocal operator," *Medical image analysis*, vol. 18, no. 6, pp. 843–856, 2014.
- [14] Julien Mairal, Francis Bach, Jean Ponce, Guillermo Sapiro, and Andrew Zisserman, "Non-local sparse models for image restoration," in *Computer Vision, 2009 IEEE 12th International Conference on*. IEEE, 2009, pp. 2272–2279.
- [15] Weisheng Dong, Guangming Shi, and Xin Li, "Nonlocal image restoration with bilateral variance estimation: a low-rank approach," *IEEE transactions on image processing*, vol. 22, no. 2, pp. 700–711, 2013.
- [16] Hojin Kim, Josephine Chen, Adam Wang, Cynthia Chuang, Mareike Held, and Jean Pouliot, "Non-local total-variation (nlTV) minimization combined with reweighted l_1 -norm for compressed sensing CT reconstruction," *Physics in Medicine and Biology*, vol. 61, no. 18, pp. 6878, 2016.
- [17] Shuhang Gu, Wangmeng Zuo, Qi Xie, Deyu Meng, Xiangchu Feng, and Lei Zhang, "Convolutional sparse coding for image super-resolution," in *Proceedings of the IEEE International Conference on Computer Vision*, 2015, pp. 1823–1831.
- [18] Shuhang Gu, Lei Zhang, Wangmeng Zuo, and Xiangchu Feng, "Weighted nuclear norm minimization with application to image denoising," in *Proceedings of the IEEE Conference on Computer Vision and Pattern Recognition*, 2014, pp. 2862–2869.
- [19] Fan Zhang, Xin Zhang, Xue-Ying Qin, and Cai-Ming Zhang, "Enlarging image by constrained least square approach with shape preserving," *Journal of Computer Science and Technology*, vol. 30, no. 3, pp. 489–498, 2015.
- [20] Stephen Boyd, Neal Parikh, Eric Chu, Borja Peleato, and Jonathan Eckstein, "Distributed optimization and statistical learning via the alternating direction method of multipliers," *Foundations and Trends® in Machine Learning*, vol. 3, no. 1, pp. 1–122, 2011.
- [21] Gene H Golub and Charles F Van Loan, *Matrix computations*, vol. 3, JHU Press, 2012.
- [22] Biswa Nath Datta, *Numerical linear algebra and applications*, Siam, 2010.
- [23] Emmanuel Candes and Justin Romberg, "l1-magic: Recovery of sparse signals via convex programming," [URL: www.acm.caltech.edu/l1magic/downloads/l1magic.pdf](http://www.acm.caltech.edu/l1magic/downloads/l1magic.pdf), vol. 4, pp. 14, 2005.
- [24] Zhou Wang, Alan Conrad Bovik, Hamid Rahim Sheikh, and Eero P Simoncelli, "Image quality assessment: from error visibility to structural similarity," *Image Processing, IEEE Transactions on*, vol. 13, no. 4, pp. 600–612, 2004.